ACS Medicinal Chemistry Letters

pubs.acs.org/acsmedchemlett Letter

Dual Glycolate Oxidase/Lactate Dehydrogenase A Inhibitors for Primary Hyperoxaluria

Jinyue Ding,* Rajesh Gumpena, Marc-Olivier Boily, Alexandre Caron, Oliver Chong, Jennifer H. Cox, Valerie Dumais, Samuel Gaudreault, Aaron H. Graff, Andrew King, John Knight, Renata Oballa, Jayakumar Surendradoss, Tim Tang, Joyce Wu, W. Todd Lowther,* and David A. Powell

Cite This: *ACS Med. Chem. Lett.* 2021, 12, 1116−1123 Read Online

ACCESS | Metrics & More | Article Recommendations | Supporting Information

ABSTRACT: Both glycolate oxidase (GO) and lactate dehydrogenase A (LDHA) influence the endogenous synthesis of oxalate and are clinically validated targets for treatment of primary hyperoxaluria (PH). We investigated whether dual inhibition of GO and LDHA may provide advantage over single agents in treating PH. Utilizing a structure-based drug design (SBDD) approach, we developed a series of novel, potent, dual GO/LDHA inhibitors. X-ray crystal structures of compound **15** bound to individual GO and LDHA proteins validated our SBDD strategy. Dual inhibitor **7** demonstrated an IC_{50} of 88 nM for oxalate reduction in an *Agxt*-knockdown mouse hepatocyte assay. Limited by poor liver exposure, this series of dual inhibitors failed to demonstrate significant PD modulation in an *in vivo* mouse model. This work highlights the challenges in optimizing *in vivo* liver exposures for diacid containing compounds and limited benefit seen with dual GO/LDHA inhibitors over single agents alone in an *in vitro* setting.

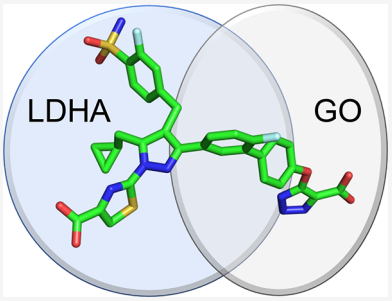

KEYWORDS: *Glycolate oxidase, Lactate dehydrogenase A, Dual inhibitors, Structure-based drug design, Primary hyperoxaluria*

Primary hyperoxaluria (PH) is a rare genetic disorder resulting in oxalate overproduction, formation of calcium oxalate kidney stones, and in some patients, end stage kidney failure.[1] There are three types of PH, 1, 2, and 3.[2] PH1 is caused by mutations in the gene *AGXT*, which encodes the alanine-glyoxylate aminotransferase (AGT) protein (Figure 1).

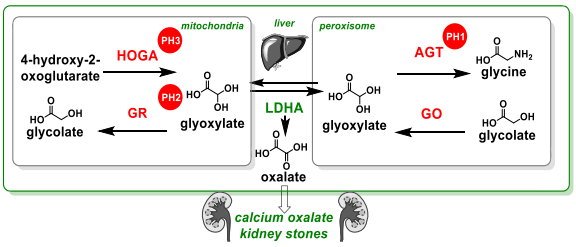

Figure 1. Metabolic pathways of oxalate synthesis.

PH2 and PH3 are caused by mutations in the genes which produce glyoxylate reductase (GR) and 4-hydroxy-2-oxoglutarate aldolase (HOGA) proteins, respectively. These mutations result in an autosomal recessive disorder of glyoxylate metabolism, impairing hepatic detoxification of glyoxylate and corresponding excessive oxalate production in the liver *via* the action of lactate dehydrogenase A (LDHA). Oxalate produced in the liver is excreted *via* the kidneys, but when present at high concentrations, it complexes with calcium to form calcium oxalate salt. Deposits of calcium oxalate within the kidney can lead to inflammation, interstitial fibrosis, tissue damage, urinary tract infections and, in severe cases, kidney failure.[3a] As kidney function deteriorates, concentrations of plasma oxalate increase, and calcium oxalate can accumulate and crystallize in other tissues such as eyes, skin, heart, bones, and brain. Two inhibition mechanisms have been the focus of therapeutic development for PH: glycolate oxidase (GO)[3] and LDHA.[4]

GO is encoded by the *HAO1* gene and expressed exclusively in the liver peroxisome in humans. As a flavin mononucleotide (FMN)-dependent α-hydroxyacid oxidase, GO converts glycolate into glyoxylate (Figure 1), resulting in increased production of oxalate *via* LDHA. PH1 patients, with deficiency in AGT, have higher levels of glycolate.[5] The Salido group reported that *Hao1*$^{-/-}$ mice developed high urinary glycolate levels but were overall healthy.[6a] Compared to *Agxt*$^{-/-}$ mice with a hyperoxaluria phenotype, *Agxt*$^{-/-}$-*Hao1*$^{-/-}$ double-knockout mice demonstrated reduced urinary oxalate levels. Additionally, **CCPST** (4-carboxy-5-[(4-chlorophenyl)-sulfanyl]-1,2,3-thiadiazole), a modestly potent GO inhibitor,

Received: April 7, 2021
Accepted: May 18, 2021
Published: May 20, 2021

https://doi.org/10.1021/acsmedchemlett.1c00196
ACS Med. Chem. Lett. 2021, 12, 1116−1123

caused oxalate reductions in a cellular *Agxt*$^{-/-}$ mouse hepatocyte assay. When administered orally to *Agxt*$^{-/-}$ mice, CCPST reduced urinary oxalate excretion by 30−50%.[6a] Clinically, lumasiran, a GalNAc-conjugated GO-siRNA therapeutic developed by Alnylam, achieved robust urinary oxalate reduction in PH1 patients.[3]

In contrast to the indirect influence of GO on oxalate production, the LDH enzymes, encoded by *LDH* A−C genes, not only catalyze the reversible conversion of pyruvate and NADH to lactate and NAD$^+$ but also convert glyoxylate to oxalate (Figure 1). Thus, inhibition of liver LDHA represents a viable approach for blocking oxalate production and, being the terminal and committed step in oxalate synthesis, may be effective in treating all three types of PH. Individuals with LDHB deficiency often do not have adverse symptoms,[7] although LDHA-deficient individuals can experience muscle-related adverse events which can lead to myoglobinuria and kidney damage.[8] Importantly, liver LDHA has been selectively targeted using the GalNAc−siRNA conjugate nedosiran from Dicerna. This approach is currently in phase 3 trials and has shown efficacy in reducing urinary oxalate levels in PH1 and PH2 patients.[4,9] This suggests that LDHA-inhibition in the liver is sufficient for reducing urinary oxalate in PH patients.

Because GO and LDHA inhibition have been validated clinically *via* GalNAc-conjugated siRNA therapeutics, we sought to investigate whether additional benefit may be obtained from a dual GO/LDHA small molecule inhibitor.[10] This would represent a novel and clinically derisked therapeutic approach for all three forms of PH. With multispecific drugs emerging as a powerful drug targeting approach in modern biopharmaceutical industry,[11] we also envisioned that a class of bispecific small molecules would further illustrate the effectiveness of target-based therapeutic molecules. To evaluate the possibility of dual GO/LDHA inhibition by a single small molecule agent, we utilized published structural data of small molecule inhibitors bound to GO and LDHA to inform our approach.

Several potent, small molecule GO inhibitors have been reported, which are defined structurally by a nonpolar tail and polar acidic warhead. The latter resembles the GO substrate, glycolate, and forms multiple key interactions with the enzyme. Examples of well-studied acidic warheads include 3-hydroxy-1*H*-pyrrole-2,5-dione,[12] 1,2,3-thiadiazole-4-carboxylic acid,[6] and 1,2,3-triazole-4-carboxylic acid[13] (Figure 2). The crystal structure of GO in complex with CDST (4-carboxy-5-dodecylsulfanyl-1,2,3-triazole; K_i 15 nM) containing a triazole carboxylic acid warhead was studied by Murray *et al.*[13a] A hybrid of **CDST** and **CCPST**, compound **A**, was synthesized and determined as a potent GO inhibitor (Figure 2). Several patented examples of potent GO inhibitors featuring a triazole acid warhead have also been described.[14] The numerous interactions between **CDST** and the GO active site are detailed in Figure 3A. Residues His260 and Tyr132 interact with the triazole ring, while Arg167 and Arg263 coordinate the acid moiety. The phenol moiety of Tyr26 has a long-range interaction with the sulfur atom of the thioether. We considered that a triazole warhead of a dual inhibitor could be utilized to engage the active site and the solvent exposed, hydrophobic tail could potentially be substituted with LDHA-inhibitor.

Given the central role of LDHA in glycolysis, LDHA inhibitors have been studied as potential therapeutics in oncology.[15] Several scaffolds with potent LDHA inhibition

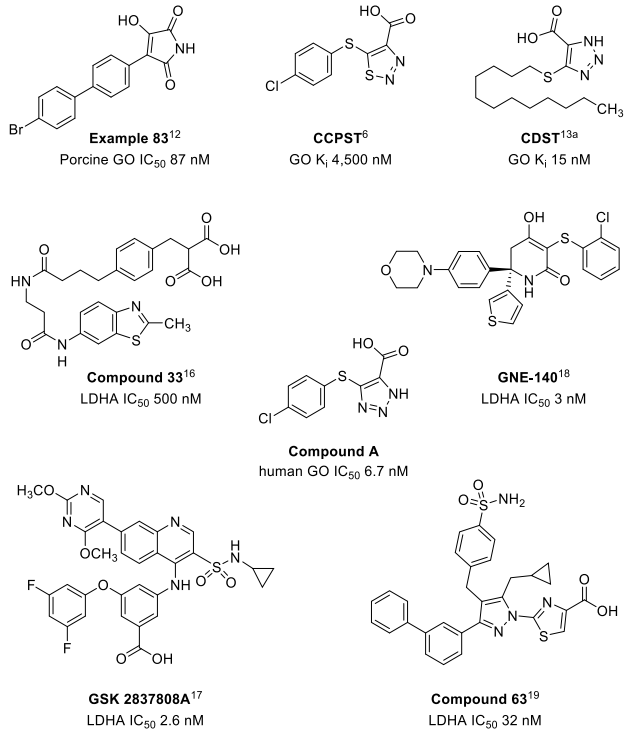

Figure 2. Representative examples of GO and LDHA inhibitors.

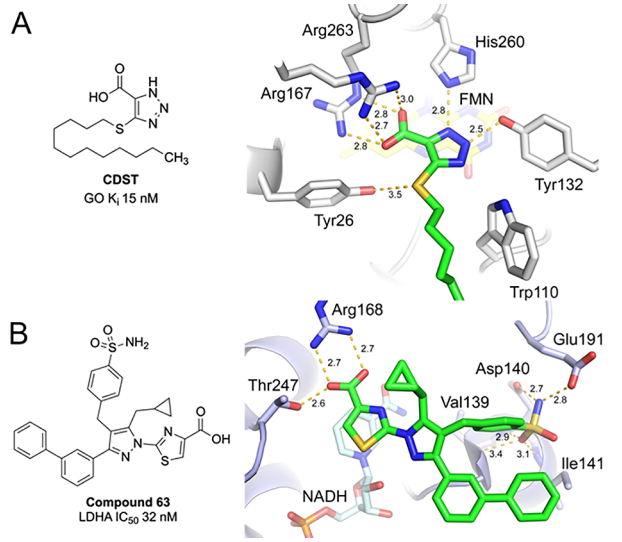

Figure 3. (A) Key interactions of GO with **CDST** (PDB 2RDT)[13a] and (B) LDHA with compound **63** (PDB 5W8L).[19a]

have been developed by pharmaceutical companies, including AstraZeneca (compound **33**),[16] GlaxoSmithKline (**GSK 2837808A**),[17] and Genentech (**GNE-140**)[18] (Figure 2). Upon examining the SAR and the crystal structures of these compounds bound to LDHA, we were intrigued by the class of pyrazole-based LDHA inhibitors and their unique binding conformation.[19] The nanomolar inhibitor compound **63** (Figure 3B) highlights three key interactions: (1) thiazole acid warhead with residue Arg168 and Thr247, (2) cyclopropyl $\pi-\pi$ interaction with Tyr238 (not shown for clarity), and (3) sulfonamide with Asp140, Glu191, and Ile141. More recently, the same group reported the beneficial impact of a 2-fluorine substituent on the benzenesulfonamide ring.[19b] Of

https://doi.org/10.1021/acsmedchemlett.1c00196
ACS Med. Chem. Lett. 2021, 12, 1116−1123

note, the terminal biphenyl tail points toward solvent-exposed area and does not form any key interactions with the LDHA enzyme.

On the basis of structural analysis of GO-**CDST** and LDHA-compound **63** complexes described above, both scaffolds contain a rather large solvent-exposed terminal moiety. Therefore, we hypothesized that upon merging the two scaffolds at the solvent-exposed fronts, a series of diacid-containing compounds may engage the required protein residues to potently inhibit both GO and LDHA (Figure 4). We sought to identify shorter linkers to minimize the overall molecular weight of the dual inhibitors and ideally maintain drug-like properties.

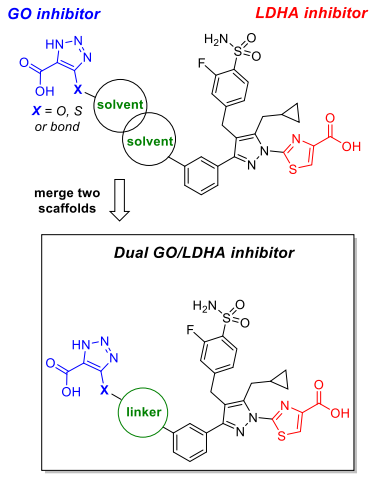

Figure 4. Strategy for the generation of dual GO/LDHA inhibitors.

On the basis of the above hypothesis, a series of compounds containing both the GO warhead (triazole acid) and LDHA warhead (thiazole carboxylic acid) were synthesized (Scheme 1). The GO warhead precursor, *N*-PMB protected triazole carboxylate **1**, was assembled following a literature method.[20] The corresponding *tert*-butyl ester **2** was obtained upon hydrolysis of ethyl ester **1** followed by treatment with di-*tert*-butyl dicarbonate. After an S_NAr reaction with 1-(3-sulfanylphenyl)ethanone, the sulfur-linked triazole carboxylate **3**, was synthesized. The acetyl group of **3** allowed further construction of the compound **63**-like scaffold, following literature procedures.[19] The acetophenone **3** underwent a magnesium bromide-catalyzed soft enolization in the presence of Hünig's base,[21] yielding 1,3-diketone **4** in 51% yield, which was then alkylated with 4-(bromomethyl)-2-fluorobenzenesulfonamide. This was followed by cyclization with hydrazine, yielding the desired pyrazole intermediate **5** in a quantitative yield. When treated with sodium *tert*-pentoxide at 0 °C, pyrazole **5** underwent a regioselective arylation reaction with ethyl 2-fluorothiazole-4-carboxylate, favoring the desired regioisomer **6**. Use of other bases and the chloro or bromo thiazole ester resulted in reduced selectivity for the desired arylated pyrazole isomer. Both *tert*-butyl and PMB protecting groups in compound **6** were removed in one step by reaction with trifluoroacetic acid and triethylsilane. Further hydrolysis of the resulting ethyl ester resulted in diacid **7**.

The corresponding oxygen linker analogue **11** (Scheme 2) was synthesized from the bromo intermediate **8**, which can be accessed in the same manner as described in Scheme 1 (steps d–g), starting from 1-(3-bromo-4-fluorophenyl)ethan-1-one.

Scheme 1. Synthesis of Analogue 7[a]

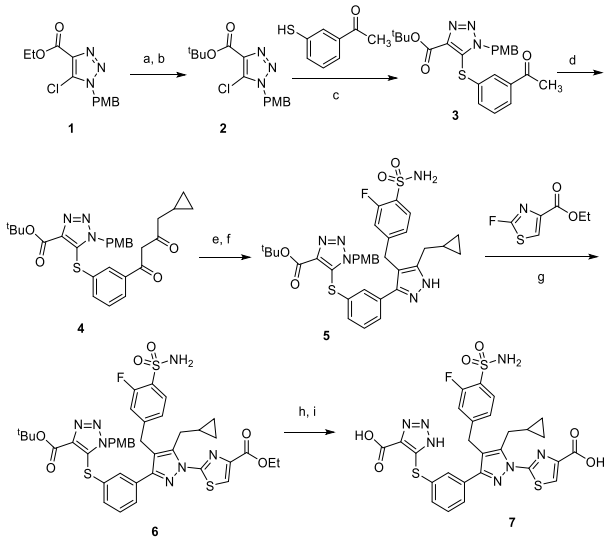

[a]Reagents and conditions: (a) LiOH, THF, H_2O, 23 °C, 4 h, 66%; (b) $(Boc)_2O$, DMAP, *i*Pr_2NEt, CH_2Cl_2, 23 °C, 3 h, 83%; (c) K_2CO_3, DMF, 130 °C, 2 h, 87%; (d) 1-(1*H*-benzo[*d*][1,2,3]triazol-1-yl)-2-cyclopropylethan-1-one, $MgBr_2{\cdot}Et_2O$, *i*Pr_2NEt, CH_2Cl_2, 23 °C, 2 h, 51%; (e) 4-(bromomethyl)-2-fluorobenzenesulfonamide, Cs_2CO_3, KI, DMSO, 23 °C, 2 h, 78%; (f) $NH_2NH_2{\cdot}H_2O$, EtOH, 70 °C, 2 h, 95%; (g) sodium *tert*-pentoxide, DMF, 0 °C, 1 h, 21%; (h) TFA, Et_3SiH, 40 °C, 18 h, 18%; (i) 1 M aqueous LiOH, THF, MeOH, 23 °C, 2 h, 45%.

Scheme 2. Synthesis of Analogue 11[a]

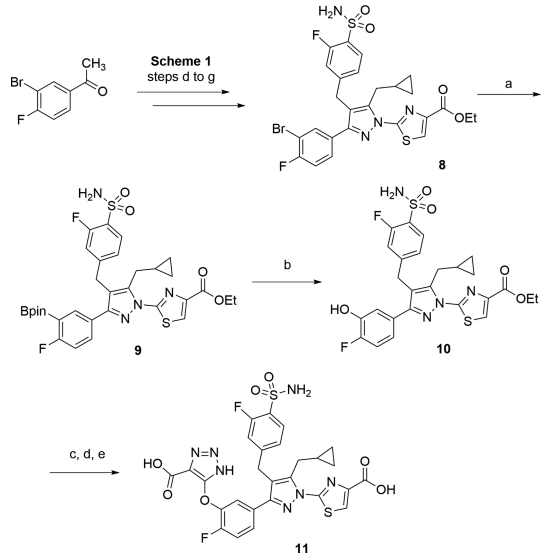

[a]Reagents and conditions: (a) $Pd(dppf)Cl_2$, B_2pin_2, KOAc, dioxane, 100 °C, 18 h, 46%; (b) urea hydrogen peroxide, MeOH, 23 °C, 18 h, 82%; (c) **2**, K_2CO_3, DMF, 130 °C, 2 h, 19%; (d) TFA, Et_3SiH, 40 °C, 18 h, 37%; (e) 1 M aqueous LiOH, THF, MeOH, 23 °C, 2 h, 53%.

The bromo intermediate **8** underwent a Miyaura borylation reaction, yielding the corresponding pinacol boronate **9**, which was further oxidized to the desired phenol intermediate **10**. After S_NAr reaction with intermediate **2**, deprotection of PMB and *tert*-butyl ester, and saponification of ethyl carboxylate, the oxygen linker analogue **11** was accessed.

https://doi.org/10.1021/acsmedchemlett.1c00196
ACS Med. Chem. Lett. 2021, 12, 1116–1123

Both sulfur and oxygen-linker analogues were further evaluated in a series of *in vitro* assays. Gratifyingly, both compounds exhibited good potency against both GO and LDHA enzymes, with IC_{50} values ranging from 0.3−11 nM (Table 1). Both compounds were further examined in a mouse primary hepatocyte assay, where hepatocytes were freshly isolated from wild-type mice (CD1 from Charles River Laboratories) and incubated with tested compound in the presence of pyruvate. Compound potency was determined by measuring inhibition of lactate production in the freshly isolated hepatocytes. Measurement of oxalate production requires ion chromatography mass spectrometry (ICMS)[22] for enhanced sensitivity. Interestingly, compound **7** was about 6-fold more potent in the mouse primary hepatocyte assay than compound **11**, while both compounds showed similar potency against mouse LDHA (mLDHA) and the human enzyme. Because this primary hepatocyte assay measures intracellular LDHA inhibition, their minor potency difference against GO would have little impact in this discrepancy. Compound **7** exhibits a 0.8 unit higher $clogD_{7.4}$ value than that of compound **11** (Table 1) and may possess higher cellular permeability, which could explain the cellular potency differences. Additionally, structural changes from compounds **7** to **11** might have an impact on LDHA binding kinetics.[19b]

Table 1. *In Vitro* Profile of First-Generation Dual GO/LDHA Inhibitors 7 and 11[a]

	enzyme IC_{50} (nM)				
compd	GO	LDHA	mLDHA	primary mouse hepatocyte IC_{50} (nM)	$clogD_{7.4}$
7	4.7	0.5	0.7	136	−0.3
11	11	0.4	0.3	732	−1.1

[a]See Supporting Information for assay conditions; $clogD_{7.4}$ values were calculated using ACD laboratories (ACD/Percepta 2014 Release). All IC_{50} values are mean values determined from more than two replicates.

Given the improved cellular LDHA inhibition of the less hydrophilic analogue **7**, we next explored the synthesis of analogues with more lipophilic moieties in the linker region (Scheme 3) with the goal of further improving the mouse hepatocyte cellular potency *via* improved permeability. The more lipophilic oxygen-linker analogue **14** was accessed in three steps, starting from a S_NAr reaction between 3-bromophenol and triazole intermediate **1** (Scheme 3). The resulting bromide **12** underwent a Pd-catalyzed Suzuki−Miyaura coupling reaction with pinacol boronate intermediate **9**, yielding the diethyl ester **13**. After PMB deprotection and ester hydrolysis, **14** was obtained in 15% yield over two steps. Three more analogues, **15**, **16**, and **17**, were synthesized in a similar manner, starting from 4-bromophenol, 4-bromothiophenol, and *tert*-butyl 5-(4-iodophenyl)-1*H*-1,2,3-triazole-4-carboxylate, respectively.

These less hydrophilic compounds, with $clogD_{7.4}$ values in the 0.6−1.2 range, exhibited subnanomolar IC_{50} values against both GO and LDHA enzymes. The direct-linked analogue **17** had an IC_{50} of 3.6 nM against GO (Table 2). Compared to the oxygen or sulfur-linker analogues, the moderately reduced potency observed in the direct-linker analogue **17** could be due to the polar hydroxyl group of Tyr26 in the GO active site (Figure 3A). Nonetheless, all four analogues demonstrated good potency (EC_{50} 143−230 nM) in a mouse hepatocyte assay, further strengthening our hypothesis between lipophilicity and cell activity for the current structural series.

Scheme 3. Synthesis of Second-Generation Dual GO/LDHA Inhibitors[a]

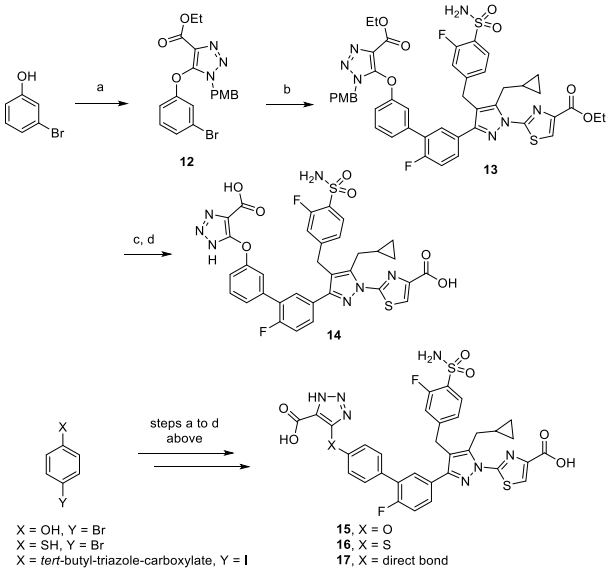

[a]Reagents and conditions: (a) **1**, K_2CO_3, DMF, 130 °C, 9 h, 93%; (b) **9**, $Pd(dppf)Cl_2$, 2 M aqueous K_3PO_4, dioxane, 130 °C, 1 h, 60%; (c) TFA, Et_3SiH, 40 °C, 18 h, 59%; (d) 1 M aqueous LiOH, THF, MeOH, 23 °C, 18 h, 25%.

Table 2. *In Vitro* Profile of Second-Generation Dual GO/LDHA Inhibitors[a]

	enzyme IC_{50} (nM)				
compd	GO	LDHA	mLDHA	primary mouse hepatocyte IC_{50} (nM)	$clogD_{7.4}$
14	0.9	0.1	0.2	143	0.6
15	1.2	0.07	0.4	198	0.6
16	1.1	0.3	0.2	230	1.2
17	3.6	0.3	0.4	170	0.7

[a]See Supporting Information for enzyme and hepatocyte assay conditions; $clogD_{7.4}$ values were calculated using ACD laboratories (ACD/Percepta 2014 Release). All IC_{50} values are mean values determined from more than two replicates.

Our strategy of utilizing a structure-based drug design (SBDD)[23] led to a series of highly potent dual GO/LDHA inhibitors. To validate the mode of binding for these novel dicarboxylic acid series, we determined the crystal structure of compound **15** in complex with GO and LDHA at 2.07 and 2.50 Å resolution (Supporting Information, Table S1), respectively. In the GO-compound **15** complex, the triazole acid warhead preserves all key interactions with residues Arg167/263, Tyr26, Trp110, Tyr132, and His260 (Figure 5A), previously observed in the GO-**CDST** complex (Figure 3A). The remainder of the compound, similar to the lipid-like tail of **CDST**, was accommodated into the solvent exposed area by loop 4 movements.[13a]

In contrast to GO, compound **15** binds to LDHA in two slightly different but well-defined conformations (Figure 5B). In both conformations, the LDHA binding regions of compound **15** were well aligned, highlighting all three binding features observed in the LDHA-compound **63** complex (Figure 3B), including thiazole acid warhead with Arg168/Thr247,

https://doi.org/10.1021/acsmedchemlett.1c00196
ACS Med. Chem. Lett. 2021, 12, 1116−1123

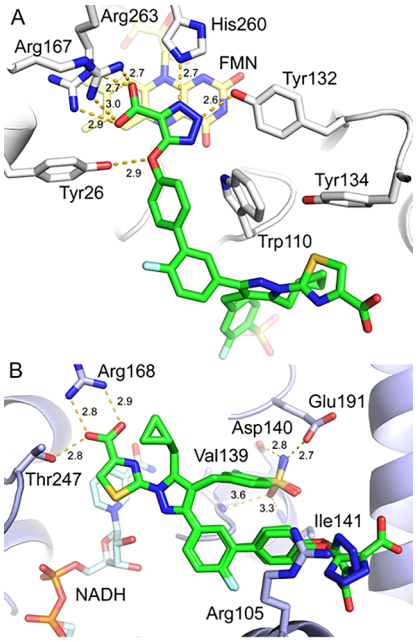

Figure 5. X-ray crystal structures of compound **15** in complex with (A) GO (PDB 7M2O) and (B) LDHA (PDB 7M2N).

cyclopropyl moiety with Tyr238 (not shown for clarity), and the sulfonamide with Asp140/Glu191/Ile141, all of which are critical for a potent LDHA inhibition. Interestingly, the terminal triazole acid GO warhead group extended toward solvent, with a ~90° rotation between conformers, demonstrating the considerable conformational freedom afforded by this region. The helix associated with Arg105 also moved outward to facilitate binding.

While the structural and chemical hypotheses proposed herein were validated with the new dual inhibitors, the question of whether the dual compound scaffold exhibits efficacy in cellular assays and animals remained. Therefore, we examined the profile of the current series of dual GO/LDHA inhibitors in a cellular model of PH1. In this assay, compound-mediated inhibition of glycolate to oxalate conversion was assessed in freshly isolated hepatocytes from mice deficient in AGT through the hepatic knockdown of the *Agxt* gene *via* an *Agxt*-siRNA encapsulated in a lipid nanoparticle (LNP) as reported in the literature.[24] Conversion of glycolate to oxalate was measured using ICMS.[22] The advantage of this lower throughput assay is the direct measurement of reduction of oxalate production from glycolate, which encompasses both GO and LDHA inhibitory pathways simultaneously (Figure 1). Seven days following a single intravenous administration of *Agxt*-siRNA LNP to CD1 mice, hepatocytes were isolated and freshly incubated with glycolate and inhibitor at various concentrations (Table 3). In this assay, compound **7** demonstrated robust inhibition of oxalate production with an IC_{50} of 88 nM, further validating the role of these dual GO/LDHA inhibitors in inhibiting oxalate synthesis, the etiological driver in PH. In the same oxalate reduction assay, compound **7** was only moderately more potent compared to individual GO inhibitor **A** or LDHA inhibitor **63**, while their corresponding intrinsic mouse GO or LDHA potency are comparable, suggesting dual GO/LDHA inhibition might not be additive or synergistic compared to individual inhibition.

Table 3. Wild-Type and *Agxt*-KD Hepatocyte Assays[a]

compd	mGO IC_{50} (nM)	mLDHA IC_{50} (nM)	mouse primary hepatocyte (pyruvate to lactate) IC_{50} (nM)	$Agxt^{KD}$ mouse primary hepatocyte (glycolate to oxalate) IC_{50} (nM)
7	7.7	0.8	136	88
A	14.6			149
63		0.1		181[b]

[a]See Supporting Information for assay conditions. All IC_{50} values are mean values determined from more than two replicates unless otherwise specified. [b]IC_{50} value from n = 1 experiment.

Encouraged by the robust inhibition in the PH1 mouse hepatocyte assay demonstrated by compound **7**, we sought to further assess the *in vivo* pharmacodynamic (PD) effect of this series of dual inhibitors. It is challenging to measure changes in urinary oxalate *in vivo* in wild-type mice, where their basal urinary oxalate is low. Measurements of urinary oxalate in *Agxt*-KD mice can be achieved but require 5+ days of compound treatment.[6a] Thus, we sought to measure plasma glycolate in wild-type mice, a convenient and noninvasive PD marker for GO inhibition, as a more acute measurement of compound PD.[25] Compound **7** and the second-generation analogue compound **14**, which showed superior potency in a mouse primary hepatocyte assay, were further evaluated in the mouse plasma glycolate-PD study. Compounds were orally administered at 100 mg/kg to C57BL/6N mice (n = 3 per group), and plasma glycolate levels were measured at 6 h after compound administration.[26] Neither of the dual inhibitors demonstrated a significant PD effect for plasma glycolate elevation (Figure 6). In comparison, compound **A** produced a 4−5-fold elevation of plasma glycolate 2 h post oral dosing.

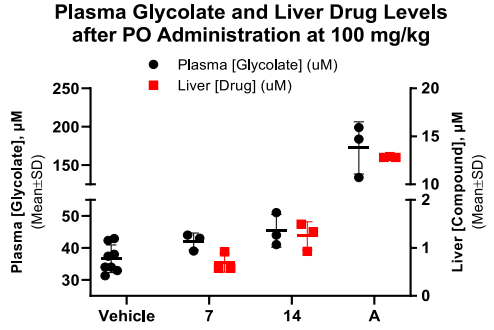

Figure 6. Mouse PK/PD of compounds **7**, **14** (6 h post oral dosing), and **A** (2 h post oral dosing).

We investigated the hepatic exposure of both compounds to understand the relationship between pharmacokinetic (PK) and the modest GO-driven PD effect. As a result, mouse liver samples were collected at the end of the PD experiment. Both dual inhibitors showed low μM liver exposures, which were significantly below liver exposures seen with compound **A** at the same dose. Poor liver exposure may be attributed to low oral absorption of the highly polar dicarboxylic acid series. Recognizing the limitations of this dicarboxylic acid series is important for further optimization and acid isosteres[27] or prodrug approaches[28] are possible strategies to improve the oral bioavailability and liver exposures.

In summary, we developed a series of potent dual GO/LDHA inhibitors utilizing a structure-based drug design strategy. The binding mode of these novel inhibitors was

https://doi.org/10.1021/acsmedchemlett.1c00196
ACS Med. Chem. Lett. 2021, 12, 1116−1123

confirmed by the X-ray crystal structures of compound **15** in complex with GO and LDHA. Careful tuning of clogD$_{7.4}$ led to a series of second-generation dual GO/LDHA inhibitors, which showed improved potency in a mouse primary hepatocyte assay, presumably *via* improved passive cellular permeability. Compound **7** demonstrated potent cellular inhibition of oxalate production in an PH1 mouse cellular model, the *Agxt*-knockdown primary hepatocyte assay. Further mouse PD studies with hepatic PK analysis revealed a limitation of the current series of dual inhibitors in reaching sufficient liver exposure to engage the hepatic GO enzyme. Finally, we were disappointed that serial inhibition of oxalate synthesis *via* dual GO/LDHA inhibition did not appear to be additive.[29] Individual novel GO or LDHA small-molecule inhibitors demonstrated similar potencies as dual inhibition in the *Agxt*-knockdown primary hepatocyte assay (50−200 nM range). Our efforts to further develop GO and LDHA small-molecule inhibitors for primary hyperoxaluria will be presented in future publications.

■ ASSOCIATED CONTENT

Supporting Information

The Supporting Information is available free of charge at https://pubs.acs.org/doi/10.1021/acsmedchemlett.1c00196.

Detailed description of chemical synthesis, ^{1}H NMR data, methods of protein expression and purification, X-ray crystallography, enzyme and hepatocyte (both wild-type and *Agxt*-knock down) assays, *in vivo* pharmacokinetic, pharmacodynamic studies, and analysis (PDF)

■ AUTHOR INFORMATION

Corresponding Authors

W. Todd Lowther − *Center for Structural Biology, Department of Biochemistry, Wake Forest School of Medicine, Winston-Salem, North Carolina 27157, United States*; Email: tlowther@wakehealth.edu

Jinyue Ding − *Chinook Therapeutics, Seattle, Washington 98102, United States*; orcid.org/0000-0003-3883-2470; Email: jding@chinooktx.com

Authors

Rajesh Gumpena − *Center for Structural Biology, Department of Biochemistry, Wake Forest School of Medicine, Winston-Salem, North Carolina 27157, United States*

Marc-Olivier Boily − *Chinook Therapeutics, Seattle, Washington 98102, United States*

Alexandre Caron − *Chinook Therapeutics, Seattle, Washington 98102, United States*

Oliver Chong − *Chinook Therapeutics, Seattle, Washington 98102, United States*

Jennifer H. Cox − *Chinook Therapeutics, Seattle, Washington 98102, United States*

Valerie Dumais − *Chinook Therapeutics, Seattle, Washington 98102, United States*

Samuel Gaudreault − *Chinook Therapeutics, Seattle, Washington 98102, United States*

Aaron H. Graff − *Center for Structural Biology, Department of Biochemistry, Wake Forest School of Medicine, Winston-Salem, North Carolina 27157, United States*

Andrew King − *Chinook Therapeutics, Seattle, Washington 98102, United States*

John Knight − *Department of Urology, University of Alabama at Birmingham, Birmingham, Alabama 35294, United States*

Renata Oballa − *Chinook Therapeutics, Seattle, Washington 98102, United States*

Jayakumar Surendradoss − *Chinook Therapeutics, Seattle, Washington 98102, United States*

Tim Tang − *Chinook Therapeutics, Seattle, Washington 98102, United States*; orcid.org/0000-0002-7055-440X

Joyce Wu − *Chinook Therapeutics, Seattle, Washington 98102, United States*

David A. Powell − *Chinook Therapeutics, Seattle, Washington 98102, United States*

Complete contact information is available at: https://pubs.acs.org/10.1021/acsmedchemlett.1c00196

Author Contributions

The manuscript was written through contributions of all authors. All authors have given approval to the final version of the manuscript.

Notes

The authors declare the following competing financial interest(s): Some authors are current or former employees of Chinook Therapeutics and potentially own and/or hold stocks in the company.

■ ACKNOWLEDGMENTS

We thank Chinook leadership team in supporting this project, Wake Forest School of Medicine (under the supervision of W.T.L.) for providing crystallization and X-ray diffraction facilities (Wake Forest Baptist Comprehensive Cancer Center P30 CA012197), and University of Alabama at Birmingham (under the supervision of J.K.) for ICMS facilities. We also thank Terrence L. Smalley for many helpful discussions.

■ ABBREVIATIONS

siRNA, small interfering RNA; GalNAc, *N*-acetylgalactosamine; NAD, nicotinamide adenine dinucleotide; PMB, *p*-methoxybenzyl; S_NAr, nucleophilic aromatic substitution; DMAP, 4-dimethylaminopyridine; DMF, dimethylformamide; DMSO, dimethyl sulfoxide; TFA, trifluoroacetic acid; LNP, lipid nanoparticle.

■ REFERENCES

(1) Lawrence, J. E.; Wattenberg, D. J. Primary Hyperoxaluria: The Patient and Caregiver Perspective. *Clin. J. Am. Soc. Nephrol.* **2020**, *15*, 909−911.

(2) (a) Raju, D. L.; Cantarovich, M.; Brisson, M.; Tchervenkov, J.; Lipman, M. L. Primary hyperoxaluria: clinical course, diagnosis, and treatment after kidney failure. *Am. J. Kidney Dis.* **2008**, *51*, e1−e5. (b) Hoppe, B. An update on primary hyperoxaluria. *Nat. Rev. Nephrol.* **2012**, *8*, 467−475. (c) Bhasin, B.; Ürekli, H. M.; Atta, M. G. Primary and secondary hyperoxaluria: Understanding the enigma. *World J. Nephrol.* **2015**, *4*, 235−244.

(3) (a) Milliner, D.; McGregor, T.; Thompson, A.; Dehmel, B.; Knight, J.; Rosskamp, R.; Blank, M.; Yang, S.; Fargue, S.; Rumsby, G.; Groothoff, J.; Allain, M.; West, M.; Hollander, K.; Lowther, W.; Lieske, J. End Points for Clinical Trials In Primary Hyperoxaluria. *Clin. J. Am. Soc. Nephrol.* **2020**, *15*, 1056−1065. (b) Liebow, A.; Li, X.; Racie, T.; Hettinger, J.; Bettencourt, B. R.; Najafian, N.; Haslett, P.; Fitzgerald, K.; Holmes, R. P.; Erbe, D.; Querbes, W.; Knight, J. An Investigational RNAi Therapeutic Targeting Glycolate Oxidase Reduces Oxalate Production in Models of Primary Hyperoxaluria. *J. Am. Soc. Nephrol.* **2017**, *28*, 494−503.

(4) Hoppe, B., Cochat, P., Lemoine, S., Lipkin, G., Gentile, A. M., Brown, B. D., Rosskamp, R., Hulton, S., Groothoff, J. W., Baum, M. A. *PHYOX: A Safety and Tolerability Study of DCR-PHXC In Primary Hyperoxaluria Types 1 and 2*; Dicerna, 2019; https://investors.dicerna.com/static-files/51c47431-1ff6-463f-8fec-67ad571da49a.
(5) (a) Frishberg, Y.; Zeharia, A.; Lyakhovetsky, R.; Bargal, R.; Belostotsky, R. Mutations in HAO1 encoding glycolate oxidase cause isolated glycolic aciduria. *J. Med. Genet.* **2014**, *51*, 526−529. (b) Craigen, W. J. Persistent glycolic aciduria in a healthy child with normal alanine-glyoxylate aminotransferase activity. *J. Inherited Metab. Dis.* **1996**, *19*, 793−794.
(6) (a) Martin-Higueras, C.; Luis-Lima, S.; Salido, E. Glycolate Oxidase Is a Safe and Efficient Target for Substrate Reduction Therapy in a Mouse Model of Primary Hyperoxaluria Type I. *Mol. Ther.* **2016**, *24*, 719−725. (b) Chen, Z. W.; Vignaud, C.; Jaafar, A.; Lévy, B.; Guéritte, F.; Guénard, D.; Lederer, F.; Mathews, F. S. High resolution crystal structure of rat long chain hydroxy acid oxidase in complex with the inhibitor 4-carboxy-5-[(4-chlorophenyl)sulfanyl]-1, 2, 3-thiadiazole. Implications for inhibitor specificity and drug design. *Biochimie* **2012**, *94*, 1172−1179. (c) Bourhis, J. M.; Vignaud, C.; Pietrancosta, N.; Guéritte, F.; Guénard, D.; Lederer, F.; Lindqvist, Y. Structure of human glycolate oxidase in complex with the inhibitor 4-carboxy-5-[(4-chlorophenyl)sulfanyl]-1,2,3-thiadiazole. *Acta Crystallogr., Sect. F: Struct. Biol. Cryst. Commun.* **2009**, *65*, 1246−1253.
(7) Tanis, R. J.; Neel, J. V.; Torres de Arauz, R. Two more "private" polymorphisms of Amerindian tribes: LDHb GUA-1 and ACP1 B GUA-1 in the Guaymi in Panama. *Am. J. Human Genetics* **1977**, *29*, 419−430.
(8) (a) Kanno, T.; Maekawa, M. Lactate dehydrogenase M-subunit deficiencies: clinical features, metabolic background, and genetic heterogeneities. *Muscle Nerve* **1995**, *18*, S54−S60. (b) Lactate dehydrogenase deficiency. *Genetic Home Reference*; U.S. National Library of Medicine, 2020; https://ghr.nlm.nih.gov/condition/lactate-dehydrogenase-deficiency.
(9) Hoppe, B., Cochat, P., Lemoine, S., Lipkin, G., Gentile, A. M., Brown, B. D., Rosskamp, R., Hulton, S., Groothoff, J. W., Baum, M. A. *PHYOX: A Safety and Tolerability Study of DCR-PHXC In Primary Hyperoxaluria Types 1 and 2*; Dicerna, **2019**; https://investors.dicerna.com/static-files/51c47431-1ff6-463f-8fec-67ad571da49a.
(10) Moya-Garzon, M. D.; Gomez-Vidal, J. A.; Alejo-Armijo, A.; Altarejos, J.; Rodriguez-Madoz, J. R.; Fernandes, M. X.; Salido, E.; Salido, S.; Diaz-Gavilan, M. Small Molecule-Based Enzyme Inhibitors in the Treatment of Primary Hyperoxalurias. *J. Pers. Med.* **2021**, *11*, 74.
(11) (a) Deshaies, R. J. Multispecific drugs herald a new era of biopharmaceutical innovation. *Nature* **2020**, *580*, 329−338. (b) Wang, Y.; Yang, S. Multispecific drugs: the fourth wave of biopharmaceutical innovation. *Sig. Transduct. Target. Ther.* **2020**, *5*, 86.
(12) Rooney, C. S.; Randall, W. C.; Streeter, K. B.; Ziegler, C.; Cragoe, E. J., Jr.; Schwam, H.; Michelson, S. R.; Williams, H. W. R.; Eichler, E.; Duggan, D. E.; Ulm, E. H.; Noll, R. M. Inhibitors of glycolic acid oxidase. 4-Substituted 3-hydroxy-1*H*-pyrrole-2,5-dione derivatives. *J. Med. Chem.* **1983**, *26*, 700−714.
(13) (a) Murray, M. S.; Holmes, R. P.; Lowther, W. T. Active Site and Loop 4 Movements within Human Glycolate Oxidase: Implications for Substrate Specificity and Drug Design. *Biochemistry* **2008**, *47*, 2439−2449. (b) Stenberg, K.; Lindqvist, Y. Three-dimensional structures of glycolate oxidase with bound active-site inhibitors. *Protein Sci.* **1997**, *6*, 1009−1015.
(14) (a) Lowther, W. T., Holmes, R. P. Glycolate oxidase inhibitors and methods of use for the treatment of kidney stones. WO2017100266A1, June 15, 2017. (b) Wang, B., Chao, Q. Glycolate Oxidase Inhibitors for the treatment of disease. WO2019133770, July 4, 2019. (c) Keller, B. T., Talley, J. J. Compounds and methods for treating oxalate related diseases, WO2019165159, August 29, 2019. (d) Maag, H., Fernandes, M. X., Zamboni, R., Akbaririomani, E., Beaulieu, M., Leblanc, Y., Thakur, P. Triazole glycolate oxidase inhibitors. WO2020010309, January 9, 2020.
(15) (a) Vander Heiden, M. G.; Cantley, L. C.; Thompson, C. B. Understanding the Warburg effect: the metabolic requirements of cell proliferation. *Science* **2009**, *324*, 1029−1033. (b) Le, A.; Cooper, C. R.; Gouw, A. M.; Dinavahi, R.; Maitra, A.; Deck, L. M.; Royer, R. E.; Vander Jagt, D. L.; Semenza, G. L.; Dang, C. V. Inhibition of lactate dehydrogenase A induces oxidative stress and inhibits tumor progression. *Proc. Natl. Acad. Sci. U. S. A.* **2010**, *107*, 2037−2042. (c) Yu, Y.; Liao, M.; Liu, R.; Chen, J.; Feng, H.; Fu, Z. Overexpression of lactate dehydrogenase-A in human intrahepatic cholangiocarcinoma: its implication for treatment. *World J. Surg. Oncol.* **2014**, *12*, 78.
(16) Ward, R. A.; Brassington, C.; Breeze, A. L.; Caputo, A.; Critchlow, S.; Davies, G.; Goodwin, L.; Hassall, G.; Greenwood, R.; Holdgate, G. A.; Mrosek, M.; Norman, R. A.; Pearson, S.; Tart, J.; Tucker, J. A.; Vogtherr, M.; Whittaker, D.; Wingfield, J.; Winter, J.; Hudson, K. Design and synthesis of novel lactate dehydrogenase A inhibitors by fragment-based lead generation. *J. Med. Chem.* **2012**, *55*, 3285−3306.
(17) Billiard, J.; Dennison, J. B.; Briand, J.; Annan, R. S.; Chai, D.; Colón, M.; Dodson, C. S.; Gilbert, S. A.; Greshock, J.; Jing, J.; Lu, H.; McSurdy-Freed, J. E.; Orband-Miller, L. A.; Mills, G. B.; Quinn, C. J.; Schneck, J. L.; Scott, G. F.; Shaw, A. N.; Waitt, G. M.; Wooster, R. F.; Duffy, K. J. Quinoline 3-sulfonamides inhibit lactate dehydrogenase A and reverse aerobic glycolysis in cancer cells. *Cancer Metab.* **2013**, *1*, 19.
(18) (a) Dragovich, P. S.; Fauber, B. P.; Corson, L. B.; Ding, C. Z.; Eigenbrot, C.; Ge, H.; Giannetti, A. M.; Hunsaker, T.; Labadie, S.; Liu, Y.; Malek, S.; Pan, B.; Peterson, D.; Pitts, K.; Purkey, H. E.; Sideris, S.; Ultsch, M.; VanderPorten, E.; Wei, B.; Xu, Q.; Yen, I.; Yue, Q.; Zhang, H.; Zhang, Z. Identification of substituted 2-thio-6-oxo-1,6-dihydropyrimidines as inhibitors of human lactate dehydrogenase. *Bioorg. Med. Chem. Lett.* **2013**, *23*, 3186−3194. (b) Boudreau, A.; Purkey, H. E.; Hitz, A.; Robarge, K.; Peterson, D.; Labadie, S.; Kwong, M.; Hong, R.; Gao, M.; Del Nagro, C.; Pusapati, R.; Ma, S.; Salphati, L.; Pang, P.; Zhou, A.; Lai, T.; Li, Y.; Chen, Z.; Wei, B.; Yen, I.; Sideris, S.; McCleland, M.; Firestein, R.; Corson, L.; Vanderbilt, A.; Williams, S.; Daemen, A.; Belvin, M.; Eigenbrot, C.; Jackson, P. K.; Malek, S.; Hatzivassiliou, G.; Sampath, D.; Evangelista, M.; O'Brien, T. Metabolic plasticity underpins innate and acquired resistance to LDHA inhibition. *Nat. Chem. Biol.* **2016**, *12*, 779−786.
(19) (a) Rai, G.; Brimacombe, K. R.; Mott, B. T.; Urban, D. J.; Hu, X.; Yang, S.; Lee, T.; Cheff, D. M.; Kouznetsova, J.; Benavides, G. A.; Pohida, K.; Kuenstner, E. J.; Luci, D. K.; Lukacs, C. M.; Davies, D. R.; Dranow, D. M.; Zhu, H.; Sulikowski, G.; Moore, W. J.; Stott, G. M.; Flint, A. J.; Hall, M. D.; Darley-Usmar, V. M.; Neckers, L. M.; Dang, C. V.; Waterson, A. G.; Simeonov, A.; Jadhav, A.; Maloney, D. J. Discovery and Optimization of Potent, Cell-Active Pyrazole-Based Inhibitors of Lactate Dehydrogenase (LDH). *J. Med. Chem.* **2017**, *60*, 9184−9204. (b) Rai, G.; Urban, D. J.; Mott, B. T.; Hu, X.; Yang, S.; Benavides, G. A.; Johnson, M. S.; Squadrito, G. L.; Brimacombe, K. R.; Lee, T. D.; Cheff, D. M.; Zhu, H.; Henderson, M. J.; Pohida, K.; Sulikowski, G. A.; Dranow, D. M.; Kabir, M.; Shah, P.; Padilha, E.; Tao, D.; Fang, Y.; Christov, P. P.; Kim, K.; Jana, S.; Muttil, P.; Anderson, T.; Kunda, N. K.; Hathaway, H. J.; Kusewitt, D. F.; Oshima, N.; Cherukuri, M.; Davies, D. R.; Norenberg, J. P.; Sklar, L. A.; Moore, W. J.; Dang, C. V.; Stott, G. M.; Neckers, L.; Flint, A. J.; Darley-Usmar, V. M.; Simeonov, A.; Waterson, A. G.; Jadhav, A.; Hall, M. D.; Maloney, D. J. Pyrazole-Based Lactate Dehydrogenase Inhibitors with Optimized Cell Activity and Pharmacokinetic Properties. *J. Med. Chem.* **2020**, *63*, 10984−11011. (c) Christov, P. P.; Kim, K.; Jana, S.; Romaine, I. M.; Rai, G.; Mott, B. T.; Allweil, A. A.; Lamers, A.; Brimacombe, K. R.; Urban, D. J.; Lee, T. D.; Hu, X.; Lukacs, C. M.; Davies, D. R.; Jadhav, A.; Hall, M. D.; Green, N.; Moore, W. J.; Stott, G. M.; Flint, A. J.; Maloney, D. J.; Sulikowski, G. A.; Waterson, A. G. Optimization of ether and aniline based inhibitors of lactate dehydrogenase. *Bioorg. Med. Chem. Lett.* **2021**, *41*, 127974. (d) LDHB potency was not profiled for the dual GO/LDHA compounds reported in this paper, however, based on reported potency profile of compound **63**, we expected all compounds to be of similar potency against LDHB.

https://doi.org/10.1021/acsmedchemlett.1c00196
ACS Med. Chem. Lett. 2021, 12, 1116−1123

(20) Buckle, D. R.; Rockell, C. J. M. Studies on *v*-triazoles. Part 4. The 4-methoxybenzyl group, a versatile *N*-protecting group for the synthesis of *N*-unsubstituted *v*-triazoles. *J. Chem. Soc., Perkin Trans. 1* **1982**, *0*, 627−630.
(21) Lim, D.; Fang, F.; Zhou, G.; Coltart, D. M. Direct Carbon−Carbon Bond Formation via Soft Enolization: A Facile and Efficient Synthesis of 1,3-Diketones. *Org. Lett.* **2007**, *9*, 4139−4142.
(22) Fargue, S.; Knight, J.; Holmes, R. P.; Rumsby, G.; Danpure, C. J. Effects of alanine:glyoxylate aminotransferase variants and pyridoxine sensitivity on oxalate metabolism in a cell-based cytotoxicity assay. *Biochim. Biophys. Acta, Mol. Basis Dis.* **2016**, *1862*, 1055−1062.
(23) (a) Reich, S. H.; Webber, S. E. Structure-based drug design (SBDD): Every structure tells a story. *Perspect. Drug Discovery Des.* **1993**, *1*, 371−390. (b) Klebe, G. Recent developments in structure-based drug design. *J. Mol. Med.* **2000**, *78*, 269−281.
(24) Harwiger, P., Vornlocher, H., Brown, J. M., Neuman, K. K. H. Defined Multi-Conjugate Oligonucleotides. WO2016205410, December 22, 2016.
(25) Dutta, C.; Avitahl-Curtis, N.; Pursell, N.; Larsson Cohen, M.; Holmes, B.; Diwanji, R.; Zhou, W.; Apponi, L.; Koser, M.; Ying, B.; Chen, D.; Shui, X.; Saxena, U.; Cyr, W. A.; Shah, A.; Nazef, N.; Wang, W.; Abrams, M.; Dudek, H.; Salido, E.; Brown, B. D.; Lai, C. Inhibition of Glycolate Oxidase With Dicer-substrate siRNA Reduces Calcium Oxalate Deposition in a Mouse Model of Primary Hyperoxaluria Type 1. *Mol. Ther.* **2016**, *24*, 770−778.
(26) The 6 h time point was chosen based on previous time course studies with GO inhibitors, where maximal plasma glycolate elevations (up to 10-fold) were determined 6 h post PO dosing.
(27) Lassalas, P.; Gay, B.; Lasfargeas, C.; James, M. J.; Tran, V.; Vijayendran, K. G.; Brunden, K. R.; Kozlowski, M. C.; Thomas, C. J.; Smith, A. B., III; Huryn, D. M.; Ballatore, C. Structure Property Relationships of Carboxylic Acid Isosteres. *J. Med. Chem.* **2016**, *59* (7), 3183−3203.
(28) (a) Rautio, J.; Kumpulainen, H.; Heimbach, T.; Oliyai, R.; Oh, D.; Järvinen, T.; Savolainen, J. Prodrugs: design and clinical applications. *Nat. Rev. Drug Discovery* **2008**, *7*, 255−270. (b) Jana, S.; Mandlekar, S.; Marathe, P. Prodrug design to improve pharmacokinetic and drug delivery properties: challenges to the discovery scientists. *Curr. Med. Chem.* **2010**, *17*, 3874−3908. (c) Najjar, A.; Najjar, A.; Karaman, R. Newly Developed Prodrugs and Prodrugs in Development; an Insight of the Recent Years. *Molecules* **2020**, *25*, 884.
(29) Yin, N.; Ma, W.; Pei, J.; Ouyang, Q.; Tang, C.; Lai, L. Synergistic and Antagonistic Drug Combinations Depend on Network Topology. *PLoS One* **2014**, *9* (4), No. e93960.

https://doi.org/10.1021/acsmedchemlett.1c00196
ACS Med. Chem. Lett. 2021, 12, 1116−1123